

Phosphorus Research Bulletin Vol. 35 (2019) pp. 048-054

## CATALYTIC ACTIVITY AND COKING RESISTANCE ON HYDROXYAPATITE FOR THE OXIDATIVE DEHYDROGENATION OF ISOBUTANE

Takuya Ehiro<sup>1\*</sup>, Satoru Dohshi<sup>1</sup>, Masahiro Katoh<sup>2</sup> and Shigeru Sugiyama<sup>2</sup>

(\*Corresponding author: ehirot@tri-osaka.jp)

<sup>1</sup>Osaka Research Institute of Industrial Science and Technology, 2-7-1 Ayumino, Izumi-shi, Osaka 594-1157 Japan.

<sup>2</sup>Department of Applied Chemistry, Graduate School of Technology, Industrial and Social Science, Tokushima University, 2-1 Minamijyousanjima-cho, Tokushima-shi, Tokushima 770-8506 Japan.

Keywords: Hydroxyapatite, Catalyst, Isobutane, Isobutene, Coking

Abstract: Hydroxyapatite (HAp) samples were prepared from precursor solutions with different Ca/P molar ratios. The HAp samples were utilized as catalysts for the oxidative dehydrogenation (ODH) of isobutane. Also, the HAp samples were characterized by N<sub>2</sub> and H<sub>2</sub>O adsorption-desorption measurements, X-ray diffraction, inductively coupled plasma optical emission spectrometry, thermogravimetry-differential thermal analyses, and temperature-programmed oxidation (TPO). The Ca/P molar ratio of the precursor solution had a major influence on the catalytic activity and coking resistance ability. The HAp catalyst prepared from the stoichiometric precursor solution [HAp (1.67)] showed the highest isobutene yield. Furthermore, the white color of HAp (1.67) remained unchanged during the ODH of isobutene, indicating the absence of coke on the surface of HAp (1.67) after the reaction and its higher coking resistance ability. The results of the TPO measurements showed that the HAp (1.67) catalyst possesses the strongest oxidation ability which is likely related to its higher coking resistance ability.

(Received Oct 7, 2019; Accepted Nov 7, 2019)

### INTRODUCTION

Light olefins (C<sub>2</sub>–C<sub>4</sub>) are the most important feedstocks (> 250 million metric tons per year) in the chemical industry<sup>1</sup>. Conventionally, they are produced from hydrocarbons via steam cracking of naphtha<sup>2</sup>. Although this process is cost-effective, it has a few disadvantages such as very large energy consumption, low selectivity, and a coking tendency due to a high temperature (>1073 K) required for the reaction<sup>2,3</sup>. Significant developments have been made in the production technologies for light olefins<sup>4</sup>. Dehydrogenation (DH) of light paraffins (C<sub>n</sub>H<sub>2n+2</sub> → C<sub>n</sub>H<sub>2n</sub> + H<sub>2</sub>) is one such technology which is widely used to produce olefins. The DH process for conversion of light paraffins to light olefins has been commercialized because of its high selectivity. However, the endothermic nature of the DH process requires a high reaction temperature (823–973 K), which leads to rapid coke deposition on the catalyst<sup>5</sup>. Coke deposition results in rapid catalyst deactivation. Therefore, an energy-consuming catalyst regeneration process must be frequently applied for removal of coke. Additionally, conversion of a light paraffin by the DH process has thermodynamic

constraints<sup>6</sup>. Hence, there is a potential for improvement in the DH process.

Oxidative dehydrogenation (ODH) of light paraffins (C<sub>n</sub>H<sub>2n+2</sub> + ½O<sub>2</sub> → C<sub>n</sub>H<sub>2n</sub> + H<sub>2</sub>O) is a promising and alternative technology for energy efficient production of light olefins. Due to the presence of oxygen gas as a reactant, the ODH process is exothermic, free from thermodynamic constraint, and has a lower reaction temperature than that required for the DH process. This results in less coke formation and an increase in the conversion of light paraffins. However, it is difficult to achieve high conversion rate and selectivity simultaneously, because a light olefin is more reactive than the corresponding paraffin.

In the present study, the ODH of isobutane to isobutene was investigated. Isobutene is a valuable chemical used for the production of polyisobutene, methyl tert-butyl ether, butyl rubber, and methyl acrylates<sup>7</sup>. Various metal oxide-based and metal-free catalysts such as chromia-based catalysts, metal pyrophosphates, polyoxometalates, carbon-based catalysts, and boron nitride catalysts have been investigated for the ODH of isobutane<sup>1,8</sup>. In our previous study, Cr-doped and un-doped calcium phosphates were investigated as catalysts for the

ODH of isobutane<sup>9</sup>. The study revealed that hydroxyapatite [HAp; Ca<sub>10</sub>(PO<sub>4</sub>)<sub>6</sub>(OH)<sub>2</sub>] can work as a catalyst and that the Ca/P molar ratio of the precursor solution can influence the catalytic activity. A heavy-metal-free HAp was investigated as a catalyst for the ODH of isobutane for the first time by our research group.

In the present study, the HAp catalysts were prepared from the precursor solutions with different Ca/P molar ratios by the co-precipitation method. Their catalytic activities were evaluated under different reaction conditions. The coking resistances were evaluated using temperature-programmed oxidation (TPO) measurements. The highest coking resistance was exhibited for the HAp (1.67) catalyst.

## MATERIALS AND METHODS

### *Materials*

Calcium nitrate tetrahydrate [Ca(NO<sub>3</sub>)<sub>2</sub>·4H<sub>2</sub>O, 98.5%], ammonium phosphate dibasic [(NH<sub>4</sub>)<sub>2</sub>HPO<sub>4</sub>, 99.0%], and 28% aqueous ammonia (NH<sub>3</sub>) were purchased from Fujifilm Wako Pure Chemical Corporation. β-type tricalcium phosphate (β-TCP) was purchased from Nacalai Tesque, Inc. Nitric acid (HNO<sub>3</sub>, 60%) was purchased from Kishida Chemical Co., Ltd. Carbon black (CB) was purchased from Sigma-Aldrich Japan, Inc. All chemicals were used as-received without further purification.

### *Catalyst preparation*

HAp was prepared by the previously reported method<sup>10</sup>. Ca(NO<sub>3</sub>)<sub>2</sub> and (NH<sub>4</sub>)<sub>2</sub>HPO<sub>4</sub> were dissolved in distilled water. The pH values of Ca(NO<sub>3</sub>)<sub>2</sub> aq. and (NH<sub>4</sub>)<sub>2</sub>HPO<sub>4</sub> aq. were adjusted to 11.25 and 10.25, respectively, by adding 28% aq. NH<sub>3</sub>. The pH-adjusted solutions were diluted with distilled water and were mixed quickly with vigorous stirring. The resulting white precipitate was filtered, washed with distilled water, and dried in air. Finally, HAp was obtained by calcination of the dried sample at 773 K for 3 h. The Ca/P molar ratios of the precursor solutions were adjusted to 1.50, 1.55, 1.62, and 1.67. The prepared HAp catalysts were denoted as HAp (*x*) (*x* = 1.50, 1.55, 1.62, and 1.67) where *x* represents the Ca/P molar ratio of the precursor solution.

### *Catalyst characterization*

The X-ray diffraction (XRD) patterns were recorded on an X-ray diffractometer (SmartLab, Rigaku Corp.) using monochromatized Cu K $\alpha$  radiation ( $\lambda$  = 0.15418 nm). N<sub>2</sub> and H<sub>2</sub>O adsorption-desorption measurements were performed using a BELSORP-maxII (MicrotracBEL Corp.)

apparatus. Prior to the N<sub>2</sub> and H<sub>2</sub>O adsorption-desorption measurements at 77 K and 298 K, respectively, the catalysts were pretreated at 473 K for 5 h in vacuum. The specific surface areas were calculated from N<sub>2</sub> and H<sub>2</sub>O adsorption isotherms by Brunauer–Emmett–Teller (BET) method<sup>11</sup>. The Ca/P molar ratios of the HAp catalysts were determined by inductively coupled plasma optical emission spectroscopy (ICP-OES, iCAP6300, Thermo Fisher Scientific K.K.) after dissolving them in aq. HNO<sub>3</sub> solution. Thermogravimetry-differential thermal analyses (TG-DTA) were performed using a STA7300 (Hitachi High-Technologies Corp.) under 200 mL/min of air flow with a heating rate of 10 K/min from 323 K to 1273 K.

Oxidation ability which can contribute to prevent coke accumulation on a catalyst was characterized by temperature-programmed oxidation (TPO) using a BELCAT II (MicrotracBEL Corp.) apparatus. Prior to the TPO measurement, each catalyst was mixed with CB by grinding them in an agate mortar. The CB contents of all the samples were adjusted to 3.0 wt%. In the TPO measurements, 50 mg of each sample (catalyst mixed with CB) was loaded into a quartz tube. The CB in each sample was oxidized to CO and CO<sub>2</sub> in a flow of 50 sccm of 5% O<sub>2</sub>/He. The sample temperature was ramped up from 323 K to 1073 K with a heating rate of 5 K/min. Produced CO and CO<sub>2</sub> were monitored using a quadrupole mass spectrometer (BELMass, MicrotracBEL Corp.). A fragment peak at *m/e* = 28 and 44 were used to monitor CO and CO<sub>2</sub>, respectively.

### *Catalytic activity testing*

The catalytic activity tests were carried out in a fixed-bed continuous flow reactor at atmospheric pressure. Each catalyst (0.25 g) was pelletized and sieved to 0.85–1.70 mm. They were fixed with quartz wool and pretreated with 12.5 mL/min of O<sub>2</sub> gas flow at 723 K for 1 h. After the pretreatment, the catalytic activity tests were performed in a flow of 15 mL/min of mixed gases of helium, isobutane, and oxygen at 723 K. Their partial pressures were adjusted to *P*(He) = 74.6 kPa, *P*(*i*-C<sub>4</sub>H<sub>10</sub>) = 14.4 kPa, and *P*(O<sub>2</sub>) = 12.3 kPa. These reaction conditions were used unless otherwise stated. Under these standard conditions, a homogeneous gas phase reaction was not observed. To investigate the effects of reaction conditions on catalytic activity, the feed ratio (*i*-C<sub>4</sub>H<sub>10</sub>/O<sub>2</sub>) was adjusted by changing *P*(*i*-C<sub>4</sub>H<sub>10</sub>) and *P*(O<sub>2</sub>). The produced gases were analyzed using an online gas chromatograph (GC-8APT, Shimadzu Corp.) equipped with a TCD. A Molecular Sieve 5A (MS 5A, 0.2 m × Φ3 mm) for O<sub>2</sub>, CH<sub>4</sub>, and CO and a Hayesep R (2.0 m × Φ3 mm) for CO<sub>2</sub>, C<sub>2</sub>, C<sub>3</sub>, and

C4 products were used as the columns. The carbon balance between the reactant and the products was within  $\pm 5\%$ . The product selectivity and isobutane conversion were calculated on a carbon basis.

## RESULTS AND DISCUSSION

### Physical and chemical properties

The XRD patterns of the prepared catalysts are shown in Figure 1. The crystalline phases were indexed to HAp single phases (PDF#01-071-5048). Hence, it was confirmed that the HAp crystals were formed from the precursors with different Ca/P ratios. The Ca/P molar ratios obtained by using ICP-OEC are slightly different from those of the corresponding precursor solutions (Table 1). However, the Ca/P molar ratios of the HAp catalysts increased with increasing ratios of the precursor solutions.

The BET specific surface areas calculated from  $N_2$  and  $H_2O$  adsorption isotherms (denoted as  $S_{N_2}$  and  $S_{H_2O}$ , respectively) are summarized in Table 2. As shown in Table 2,  $S_{N_2}$  and  $S_{H_2O}$  are found to be comparable, resulting in the similar  $S_{H_2O}/S_{N_2}$  ratios. It has been reported that  $S_{H_2O}$  decreases as hydrophobicity of a sample increases<sup>12-14</sup>. Therefore, hydrophilic-hydrophobic properties were evaluated from the  $S_{H_2O}/S_{N_2}$  ratios. The similar  $S_{H_2O}/S_{N_2}$  ratios indicated that the obtained HAp catalysts possessed the similar hydrophilic-hydrophobic properties.

TG-DTA curves of the HAp catalysts are shown in Figure 2. All the catalysts showed gradual weight loss probably due to the evaporation of adsorbed and structurally incorporated water. In addition, the non-stoichiometric HAp catalysts showed the sharp weight losses around 1073 K. Since the corresponding DTA signals indicated endothermic changes, the thermal decomposition of non-stoichiometric HAp to TCP may have occurred. Moreover, the sharp weight losses at around 1073 K were smaller as the Ca/P molar ratios increased. These results indicated the highest thermal stability of HAp (1.67). Because the total weight losses of all the catalysts up to 1273 K were very little (4–5%), it was considered that the present HAp catalysts possessed enough thermal stability for the ODH of isobutane at 723 K.

### Catalytic activity

The catalytic activities of the HAp catalysts are shown in Figure 3. As confirmed in the previous study<sup>9</sup>, HAp (1.67) showed the lowest  $CO_x$  selectivity and the highest isobutene selectivity during 6.0 h on-stream [Figure 3 (d)]. This catalytic behavior was

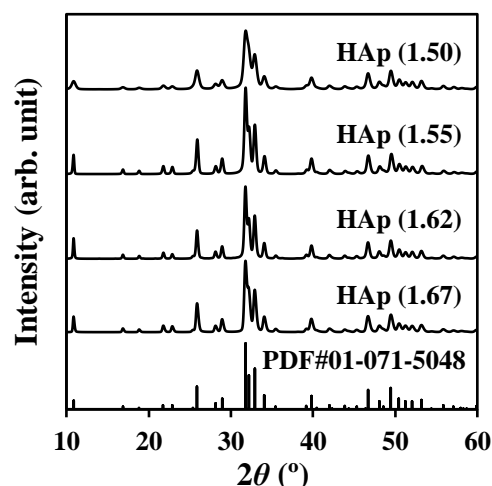


FIGURE 1 XRD patterns of the HAp catalysts.

TABLE 1 The Ca/P molar ratios of the HAp catalysts determined by ICP-OEC.

Catalyst	Ca to P molar ratio
HAp(1.50)	1.55
HAp(1.55)	1.57
HAp(1.62)	1.63
HAp(1.67)	1.66

TABLE 2 The BET specific surface areas of the HAp catalysts calculated from  $N_2$  and  $H_2O$  adsorption isotherms.

Catalyst	BET specific surface area		
	(m <sup>2</sup> /g)		$S_{H_2O}/S_{N_2}$
	$S_{N_2}$ <sup>a</sup>	$S_{H_2O}$ <sup>b</sup>	
HAp (1.50)	88	77	0.87
HAp (1.55)	81	77	0.96
HAp (1.62)	83	79	0.95
HAp (1.67)	81	75	0.93

<sup>a</sup> BET specific surface area calculated from  $N_2$  adsorption isotherm

<sup>b</sup> BET specific surface area calculated from  $H_2O$  adsorption isotherm

different from those on the other non-stoichiometric HAp catalysts. The non-stoichiometric HAp catalysts produced more  $CO_x$  and less isobutene [Figures 3 (a)–(c)]. Although HAp (1.62) showed a high isobutene selectivity at 0.75 h on-stream, it dropped thereafter without a significant decrease in isobutane conversion. Therefore, the Ca/P molar ratio around 1.63 seems to be the threshold value for the relatively high catalytic activity. On the contrary, the formation of the other products such as propylene were much less than those of  $CO_x$  and isobutene in these catalytic

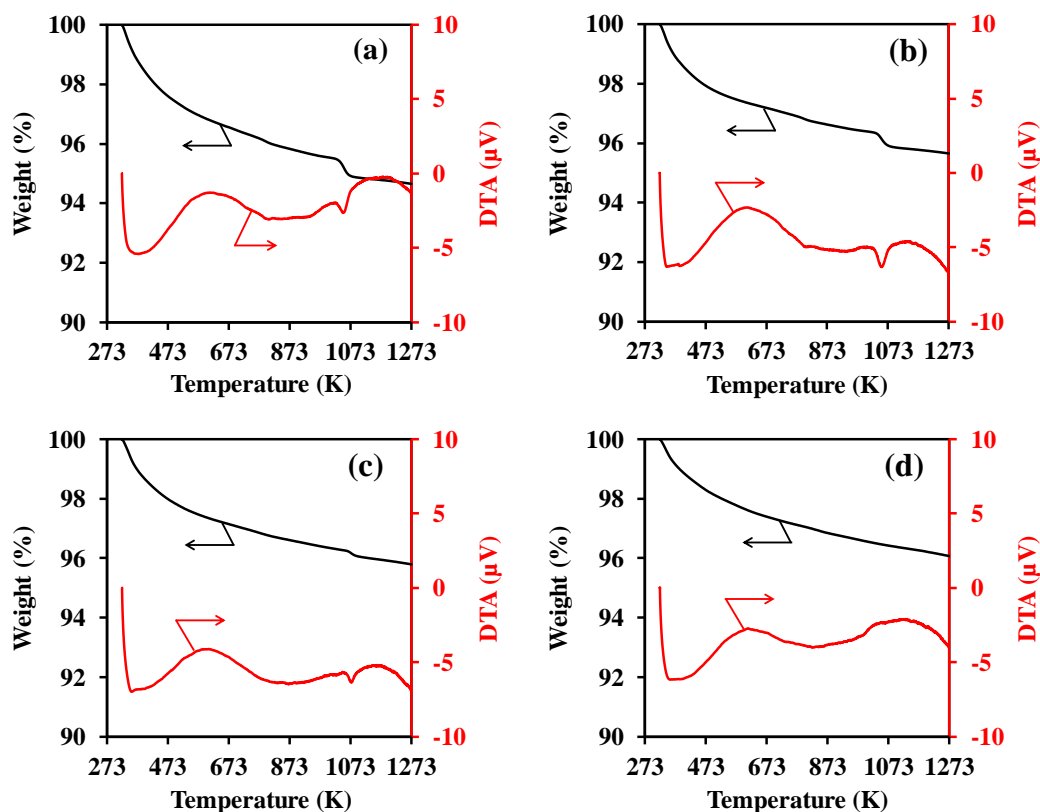


FIGURE 2 TG-DTA curves of (a) HAp (1.50), (b) HAp (1.55), (c) HAp (1.62), and (d) HAp (1.67).

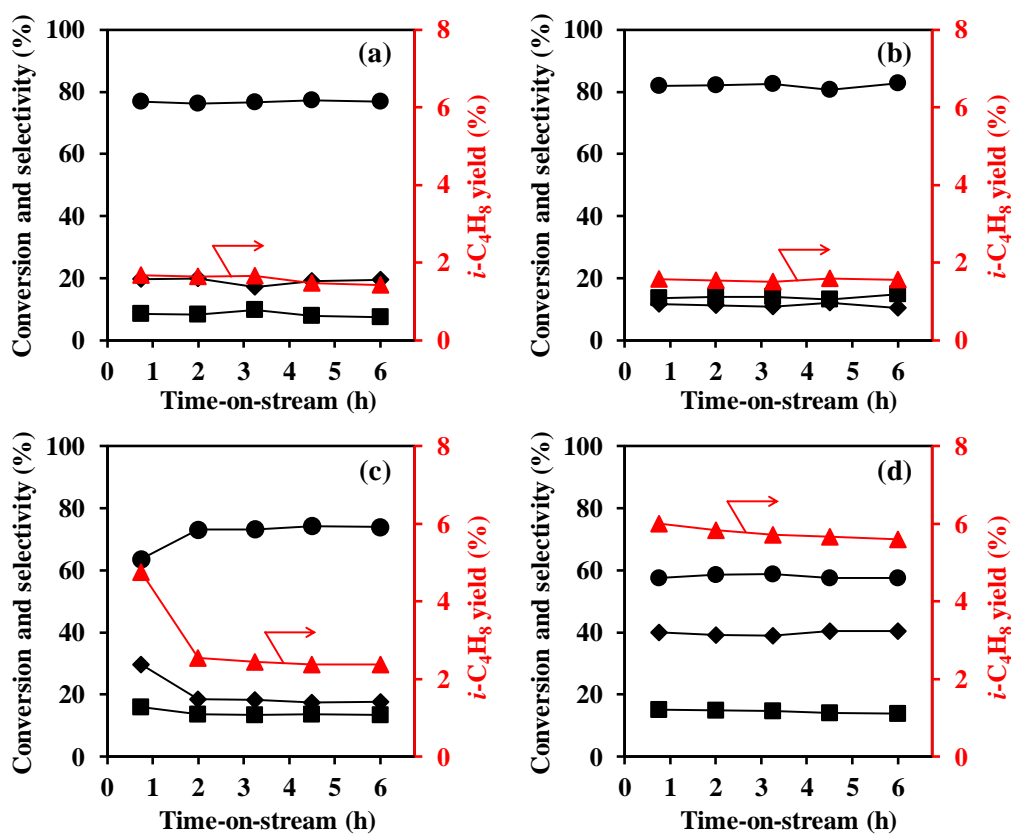


FIGURE 3 Time courses of isobutane conversions (■),  $\text{CO}_x$  selectivities (●), isobutene selectivities (◆), and isobutene yields (▲) of (a) HAp(1.50), (b) HAp(1.55), (c) HAp(1.62), and (d) HAp(1.67) under the standard reaction conditions.

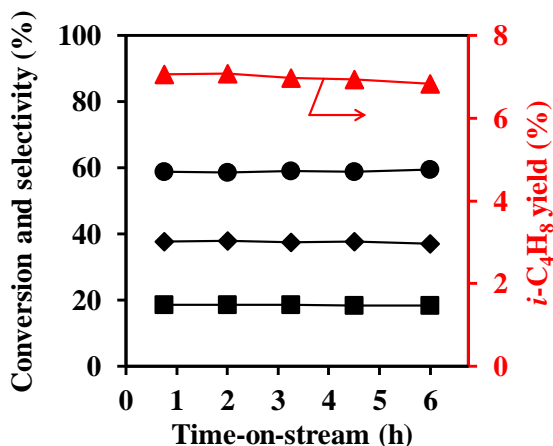


FIGURE 4 Time course of isobutane conversion (■), CO<sub>x</sub> selectivity (●), isobutene selectivity (◆), and isobutene yield (▲) of 0.5 g of HAp(1.67) under the standard conditions.

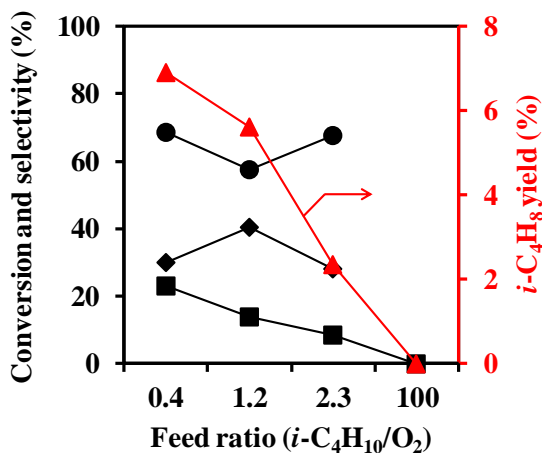


FIGURE 5 Isobutane conversion (■), CO<sub>x</sub> selectivity (●), isobutene selectivity (◆), and isobutene yield (▲) of HAp(1.67) for the ODH of isobutane at different *i*-C<sub>4</sub>H<sub>10</sub>/O<sub>2</sub> feed ratios and 6.0 h on-stream.

systems. From these results, it was revealed that the Ca/P molar ratio of the precursor solution significantly influenced the catalytic activity for the ODH of isobutane.

On the other hand, β-TCP showed the lowest isobutane conversion (2.5%) at 6.0 h on-stream under the standard reaction conditions. Therefore, it is essential for the conversion of isobutane to form the HAp crystalline structure.

To investigate the effects of the catalyst amount on the catalytic activity, 0.25 g or 0.5 g of the HAp (1.67) catalyst is loaded and tested in the reactor for

the ODH of isobutene [Figures 3 (d) and 4]. A different catalyst amount changes space velocity, which is defined as feed flow rate divided by catalyst amount. When using a higher catalyst amount, space velocity is slower. In other words, contact time of reactants is longer, enhancing the frequency to convert reactants. However, produced gases such as isobutene can also be converted more frequently at the same time. Under the present reaction conditions, it was revealed that utilizing 0.5 g of HAp (1.67) resulted in the higher isobutane conversion. This is because an increase in the amount of the catalyst makes available more active sites for the ODH of isobutane. On the other hand, the decrease in isobutene selectivity was slight. The decrease in isobutene selectivity was probably due to the consecutive conversion of isobutene. Hence, a deep oxidation of isobutene to CO<sub>x</sub> may be suppressed by the relatively strong basicity of HAp (1.67), as stated below. Consequently, a higher isobutene yield (ca. 7%) was obtained during the catalytic activity testing, by loading 0.5 g of HAp (1.67). Despite the absence of heavy metal, isobutene yield of HAp (1.67) was comparable to those of Cr-containing catalysts<sup>9,15,16</sup>.

As shown in Figure 5, isobutane conversion on HAp (1.67) decreases as the *i*-C<sub>4</sub>H<sub>10</sub>/O<sub>2</sub> feed ratio increases. These results showed that the reactivities of the reactants were increased due to the presence of oxygen. The highest isobutene selectivity was obtained at the *i*-C<sub>4</sub>H<sub>10</sub>/O<sub>2</sub> feed ratio of 1.2 while CO<sub>x</sub> selectivity was found to be the lowest. At the *i*-C<sub>4</sub>H<sub>10</sub>/O<sub>2</sub> feed ratio of 100, no isobutane conversion was observed for HAp (1.67). This behavior differs from that confirmed on the Cr-containing catalyst (Cr-MCM-41)<sup>16</sup>. With an increase in the *i*-C<sub>4</sub>H<sub>10</sub>/O<sub>2</sub> feed ratio, isobutane conversion on Cr-MCM-41 decreased while the isobutene selectivity increased monotonically<sup>16</sup>. In addition, Cr-MCM-41 produced isobutene under the oxygen lean reaction conditions. Furthermore, Cr-based catalysts are commercially utilized for the DH process<sup>17</sup> and they can produce isobutene in the absence of oxygen at an initial reaction period. On the contrary, HAp (1.67) did not convert isobutane to isobutene under the oxygen lean conditions. Considering these different catalytic behaviors, a certain amount of oxygen may have been necessary for HAp (1.67) to catalyze the ODH of isobutane.

#### Coking resistance

Although coke formation on a catalyst is less likely to occur in the ODH of isobutane compared to the case of the DH, it often occurs to some extent. Coke formation can be confirmed visually because it changes the color of a catalyst to black. In the present

study, it was confirmed that the white color of HAp (1.50), HAp (1.55), and HAp (1.62) changed to light black after the reaction. However, the color change is not observed for HAp (1.67) (Figure 6). The results indicate that the Ca/P molar ratio of the precursor solution had an influence on the coking resistance of the HAp catalyst.

To investigate the coking resistances of the HAp catalysts, their oxidation abilities were evaluated by TPO measurements. In the TPO measurements, the amounts of CO and CO<sub>2</sub> produced due to the combustion of CB were monitored. As shown in Figure 7, the CB is oxidized to CO<sub>2</sub> at a higher temperature. By physically mixing CB with the HAp catalysts, the oxidation temperatures were shifted toward a lower temperature region. Moreover, the oxidation temperatures of the HAp catalysts were lower than that of a mesoporous silica mixed with 3.0 wt% CB (not shown). Therefore, it was confirmed that the HAp catalysts promoted the oxidation of CB at a lower temperature. The compositions (mol%) of CO and CO<sub>2</sub> for all the HAp samples are summarized in Table 3. HAp (1.67) oxidized 80.3% of CB to CO<sub>2</sub>. The results indicated that the oxidation ability of HAp (1.67) was the strongest among the HAp catalysts. However, in our previous study<sup>9</sup>, it was confirmed by hydrogen temperature-programmed reduction (H<sub>2</sub>-TPR) measurements that HAp (1.67) exhibited a poor reducibility. Hence, the mechanism of the CB combustion on the HAp catalyst would be different from that on a conventional metal oxide catalyst with a mixed valence state such as CeO<sub>2</sub> whose reducibility can be confirmed by H<sub>2</sub>-TPR<sup>18</sup>.

As mentioned above, the results of the N<sub>2</sub>- and H<sub>2</sub>O-adsorption measurements indicated similar hydrophilic-hydrophobic properties of the HAp catalysts. Hence, it was speculated that the HAp catalysts have similar affinities with carbon.

According to the previously reported papers<sup>19,20</sup>,

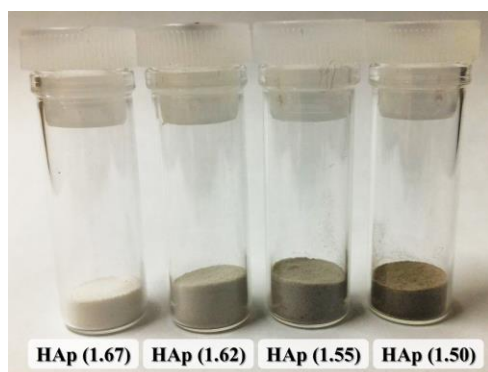


FIGURE 6 Picture of the used HAp catalysts after the ODH of isobutane under the standard reaction conditions.

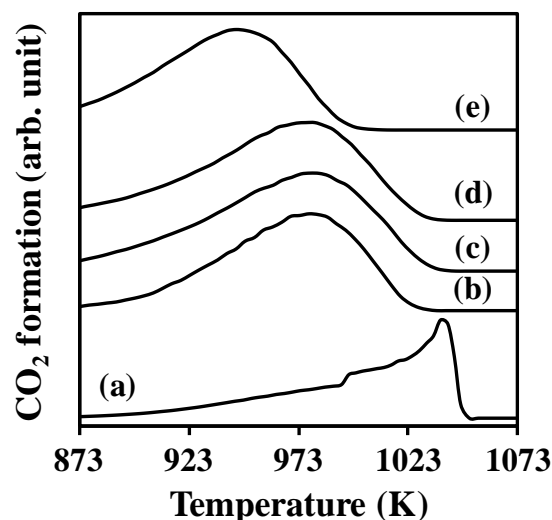


FIGURE 7 The normalized TPO spectra of (a) CB, (b) 3.0 wt% CB/HAp (1.50), (c) 3.0 wt% CB/HAp (1.55), (d) 3.0 wt% CB/HAp (1.62), and (e) 3.0 wt% CB/HAp (1.67).

TABLE 3 Composition of CO<sub>x</sub> formed during the TPO measurements.

Sample	CO <sub>x</sub> formation (mol%)	
	CO	CO <sub>2</sub>
CB	62.1	37.9
3.0 wt% CB/HAp (1.50)	60.7	39.3
3.0 wt% CB/HAp (1.55)	49.6	50.4
3.0 wt% CB/HAp (1.62)	44.8	55.2
3.0 wt% CB/HAp (1.67)	19.7	80.3

the oxidation abilities of the HAp catalysts may have been induced by the thermally generated free radicals on the HAp catalysts. At a relatively high temperature, the free radicals generated on the HAp samples were monitored by electron spin resonance spectroscopy<sup>19,20</sup>. Also, the oxidative decomposition abilities of HAp to decompose organic compounds at a relatively high temperature have been reported. The stoichiometric HAp possessed more free radicals and stronger oxidative decomposition ability at a relatively high temperature than the non-stoichiometric HAp<sup>19</sup>. In the present study, HAp (1.67) shows a stronger coking resistance than the non-stoichiometric HAp catalysts (Figures 6 and 7, Table 3). Hence, the free radicals which were thermally generated on the HAp catalyst may have prevented coke accumulation on the surface through an oxidative decomposition of coke. Therefore, it was inferred that the highest coking resistance and thermal stability could contribute to prolonging the catalyst life of HAp (1.67), preventing the rapid coke deposition and catalyst deactivation.

Although it was confirmed that HAp (1.67) strongly oxidized CB in the TPO measurements, HAp (1.67) showed the lowest CO<sub>x</sub> selectivity and the highest isobutene selectivity, compared to those of the other HAp catalysts (Figure 3). The above results can be explained by considering the basicities of isobutene and HAp (1.67). As reported in the previous study<sup>9</sup>, it was revealed that HAp (1.67) possessed the greater number of the stronger basic sites than the non-stoichiometric HAp catalysts. The stronger basicity of HAp (1.67) was considered to promote a faster desorption of isobutene which is more basic than isobutane owing to its high electron density at the  $\pi$  bond<sup>21,22</sup>. As a result, it was considered that isobutene was less likely to be oxidized on the surface of HAp (1.67), though it showed the highest coking resistance.

### CONCLUSIONS

The HAp catalysts obtained by the co-precipitation method were tested for the oxidative dehydrogenation of isobutane. Among the obtained HAp catalysts, HAp (1.67) prepared from the stoichiometric precursor solution showed the highest isobutene yield. When 0.5 g of HAp (1.67) was used, a high isobutene yield (ca. 7%) was obtained during 6.0 h on-stream. The highest isobutene selectivity (40%) was obtained on HAp (1.67) at the *i*-C<sub>4</sub>H<sub>10</sub>/O<sub>2</sub> feed ratio of 1.2. The Ca/P molar ratio of the precursor solution had a major influence on the coking resistance of the HAp catalyst as well as catalytic activity. Since the white color of the HAp (1.67) catalyst remained unchanged after the ODH of isobutane, it was revealed that coke accumulation did not take place on HAp (1.67). The TPO measurements indicated that HAp (1.67) possesses the strongest oxidation ability which is likely related to its high coking resistance ability.

### REFERENCES

1. L. Shi, Y. Wang, B. Yan, W. Song, D. Shao, A. H. Lu, *Chem. Commun.*, **54**, 10936 (2018).
2. Y. Honda, A. Takagaki, R. Kikuchi, S. T. Oyama, *Chem. Lett.*, **47**, 1090 (2018).
3. J. P. Bortolozzi, R. Portela, P. Ávila, V. Milt, E. Miro, *Catalysts*, **7**, 331 (2017).
4. I. Amghizar, L. A. Vandewalle, K. M. Van Geem, G. B. Marin, *Engineering*, **3**, 171 (2017).
5. J. M. Venegas, J. T. Grant, W. P. McDermott, S. P. Burt, J. Micka, C. A. Carrero, I. Hermans, *ChemCatChem*, **9**, 2118 (2017).
6. F. Cavani, N. Ballarini, A. Cericola, *Catal. Today*, **127**, 113 (2007).
7. C. Wei, F. Xue, C. Miao, Y. Yue, W. Yang, W. Hua, Z. Gao, *Catalysts*, **6**, 171 (2016).
8. W. Qi, D. Su, *ACS Catal.*, **4**, 3212 (2014).
9. T. Ehiro, H. Misu, S. Nitta, Y. Baba, M. Katoh, Y. Katou, W. Ninomiya, S. Sugiyama, *J. Chem. Eng. Jpn.*, **50**, 122 (2017).
10. E. Hayek, H. Newesely, *Inorg. Syntheses*, **7**, 63 (1963).
11. S. Brunauer, P. H. Emmett, E. Teller, *J. Am. Chem. Soc.*, **60**, 309 (1938).
12. F. H. Healey, Y. F. Yu, J. J. Chessick, *J. Phys. Chem.*, **59**, 399 (1955).
13. K. Boki, S. Ohno, *J. Food Sci.*, **56**, 125 (1991).
14. C. Ooka, H. Yoshida, K. Suzuki, T. Hattori, *Chem. Lett.*, **32**, 896 (2003).
15. T. Ehiro, A. Itagaki, M. Kurashina, M. Katoh, K. Nakagawa, Y. Katou, W. Ninomiya, S. Sugiyama, *J. Ceram. Soc. Jpn.*, **123**, 1084 (2015).
16. T. Ehiro, A. Itagaki, H. Misu, M. Kurashina, K. Nakagawa, M. Katoh, Y. Katou, W. Ninomiya, S. Sugiyama, *J. Chem. Eng. Jpn.*, **49**, 136 (2016).
17. B. V. Vora, *Top. Catal.*, **55**, 1297 (2012).
18. K. Nakagawa, T. Ohshima, Y. Tezuka, M. Katayama, M. Katoh, S. Sugiyama, *Catal. Today*, **246**, 67 (2015).
19. H. Nishikawa, T. Oka., N. Asai, H. Simomichi, T. Shirai, M. Fuji, *Appl. Surf. Sci.*, **28**, 5370 (2012).
20. Y. Xin, H. Ikeuchi, J. Hong, H. Nishikawa, T. Shirai, *J. Ceram. Soc. Jpn.*, **127**, 263 (2019).
21. J. Deng, L. Zhang, C. Liu, Y. Xia, H. Dai, *Catal. Today*, **164**, 347 (2011).
22. L. Zhang, J. Deng, H. Dai, C. T. Au, *Appl. Catal. A-Gen.*, **354**, 72 (2009).